Inorg. Chem. **2007**, *46*, 6215–6217

Two Frustrated, Bitetrahedral Single-Molecule Magnets

Constantinos J. Milios,[†] Ian A. Gass,[†] Alina Vinslava,[‡] Laura Budd,[†] Simon Parsons,[†] Wolfgang Wernsdorfer,[§] Spyros P. Perlepes,[#] George Christou,[‡] and Euan K. Brechin*[,†]

School of Chemistry, The University of Edinburgh, West Mains Road, EH9 3JJ Edinburgh, U.K., Department of Chemistry, University of Florida, Gainesville, Florida 32611-7200, Laboratoire Louis Néel-CNRS, 38042 Grenoble Cedex 9, France, and Department of Chemistry, University of Patras, 26504 Patras, Greece

Received April 6, 2007

Two unusual mixed-valent $\{Mn^{III}_6Mn^{II}\}$ bitetrahedra display frustrated magnetic exchange, leading to $S = {}^{13}/_2 \pm 1$ and ${}^{11}/_2 \pm 1$ ground states and slow magnetization relaxation.

We recently initiated studies into the coordination chemistry of substituted salicylaldoxime ($saoH_2$) ligands.[1−5] Much of the motivation for this project arose from the unusual discovery of ferromagnetic exchange in an oxo-centered triangular Mn^{III} single-molecule magnet (SMM) based on oximato ligands.[6] We later discovered a method for modifying the exchange interactions (antiferromagnetic → ferromagnetic) in a family of hexametallic Mn^{III} clusters, which allowed us to switch the ground-state spin values from $S =$ 4 to 12 in the molecules $[Mn^{III}_6O_2(Et\text{-}sao)_6(O_2CPh)_2(EtOH)_4(H_2O)_2]$ (**1**) and $[Mn^{III}_6O_2(Et\text{-}sao)_6(O_2CPh(Me)_2)_2(EtOH)_6]$ (**2**), which display effective energy barriers to magnetization reversal (U_{eff}) of ≤86 K.[5]

Because all known $Mn/R'CO_2^-/R\text{-}sao^{2-}$ clusters are neutral and in an attempt to further exploit the exciting $Mn/R\text{-}saoH_2$ system, we wondered if ionic complexes could be isolated. Herein we report the syntheses, structures, and magnetic properties of two new and unusual anionic heptametallic $[Mn^{III}_6Mn^{II}]$ bitetrahedra featuring the Et-sao^{2-} ligand. $Mn(O_2CMe)_2\cdot4H_2O$ (490 mg, 2 mmol), Et-$saoH_2$ (330 mg, 2 mmol), and $(NH_4)_2Ce(NO_3)_6$ (548 mg, 1 mmol) were stirred in MeCN (20 mL) for a period of 45 min. The solution was then filtered and allowed to stand. Black crystals of $(NH_4)_2[Mn_7O_2(O_2CMe)_6(Et\text{-}sao)_6]\cdot8MeCN$ (**3**·8MeCN) formed during 4 days in ∼30% yield; the complex crystallizes in the monoclinic space group $P2_1/n$. Complex $(NMe_4)[Mn_7O_2(O_2CMe)_5(Et\text{-}sao)_6(EtOH)_{0.75}(H_2O)_{1.25}]\cdot0.25H_2O$ (**4**·0.25H_2O) was synthesized by the reaction of $Mn(O_2CMe)_2\cdot4H_2O$ (245 mg, 1 mmol), Et-$saoH_2$ (165 mg, 1 mmol), and NMe_4NO_3 (136 mg, 1 mmol) in EtOH (15 mL). Crystals of **4** formed after 1 day in ∼45% yield. The core of **3** (Figures 1 and 2) consists of a bitetrahedron of seven Mn ions arranged in such a way that the two peripheral $[Mn^{III}_3O]^{7+}$ triangles are each bonded to a central Mn^{II} ion (Mn4). This ion is linked to each triangle via three fully deprotonated Et-sao^{2-} ligands in a $\eta^2{:}\eta^1{:}\eta^1{:}\mu_3$ fashion. The Mn ions in each triangle are linked to each other via one μ_3-O^{2-} ion, three $\eta^1{:}\eta^1{:}\mu$-acetates, and the three oximates via the N−O moieties to form a $[Mn^{III}_6Mn^{II}(\mu_3\text{-}O^{2-})_2(\mu_3\text{-}ON)_6]^{10+}$ core. Complex **4** also crystallizes in the monoclinic space group $P2_1/n$, and its structure is similar to that of complex **3**: two $[Mn^{III}_3O]^{7+}$ triangles linked to a central Mn^{II} ion (Mn7) giving a $[Mn^{III}_6Mn^{II}(\mu_3\text{-}O^{2-})_2(\mu\text{-}O)_6]^{10+}$ core, but now the central bridging occurs via three $\eta^2{:}\eta^2{:}\mu_3$-$MeCO_2^-$ ligands and not via the oximate ligands.

The oximate ligands bridge in a $\eta^1{:}\eta^1{:}\eta^1{:}\mu$ fashion between Mn^{III} ions along each edge of the $[Mn^{III}_3O]$ triangles. The two remaining carboxylates "cap" each triangular unit, bridging Mn1/Mn2 and Mn4/Mn6 in a $\eta^1{:}\eta^1{:}\mu$ fashion. Complexes **3** and **4** are only the second and third structurally characterized $Mn^{III}_6Mn^{II}$ clusters. The first, $[Mn_7O_4(O_2CMe)_8(trine)_2(dien)_2](PF_6)_4$ (where trine = triethylenetetramine and dien = diethylenetriamine), describes two mixed-valent $[Mn^{III}_3Mn^{II}(\mu_3\text{-}O)_2]^{7+}$ "butterflies" sharing a central Mn^{II} ion.[7]

* To whom correspondence should be addressed. E-mail: ebrechin@staffmail.ed.ac.uk.
[†] The University of Edinburgh.
[‡] University of Florida.
[§] Laboratoire Louis Néel-CNRS.
[#] University of Patras.

(1) (a) Chaudhuri, P. *Coord. Chem. Rev.* **2003**, *243*, 143. (b) Smith, A. G.; Tasker, P. A.; White, D. J. *Coord. Chem. Rev.* **2003**, *241*, 61.
(2) Milios, C. J.; Raptopoulou, C. P.; Terzis, A.; Lloret, F.; Vicente, R.; Perlepes, S. P.; Escuer, S. *Angew. Chem., Int. Ed.* **2004**, *43*, 210.
(3) Milios, C. J.; Vinslava, A.; Whittaker, A. G.; Parsons, S.; Wernsdorfer, W.; Christou, G.; Perlepes, S. P.; Brechin, E. K. *Inorg. Chem.* **2006**, *45*, 5272.
(4) Milios, C. J.; Vinslava, A.; Wood, P. A.; Parsons, S.; Wernsdorfer, W.; Christou, G.; Perlepes, S. P.; Brechin, E. K. *J. Am. Chem. Soc.* **2007**, *129*, 8.
(5) Milios, C. J.; Vinslava, A.; Wernsdorfer, W.; Moggach, S.; Parsons, S.; Perlepes, S. P.; Christou, G.; Brechin, E. K. *J. Am. Chem. Soc.* **2007**, *129*, 2754.
(6) Stamatatos, Th. C.; Foguet-Albiol, D.; Stoumpos, C. C.; Raptopoulou, C. P.; Terzis, A.; Wernsdorfer, W.; Perlepes, S. P.; Christou, G. *J. Am. Chem. Soc.* **2005**, *127*, 15380.
(7) Bhula, R.; Weatherburn, D. C. *Angew. Chem., Int. Ed. Engl.* **1991**, *30*, 688.

10.1021/ic7006638 CCC: $37.00
Published on Web 07/03/2007

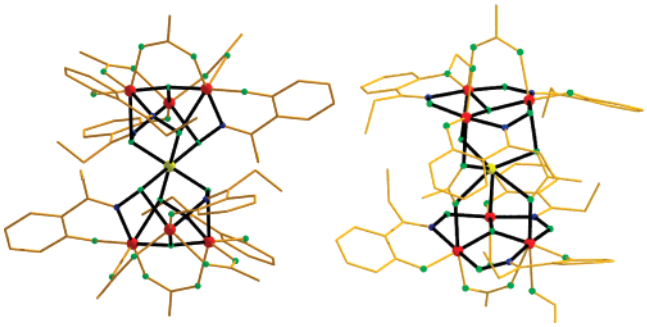

Figure 1. Molecular structures of the anions of complexes **3** (left) and **4** (right). Color code: Mn^{III}, red; Mn^{II}, yellow; O, green; N, blue; C, gold.

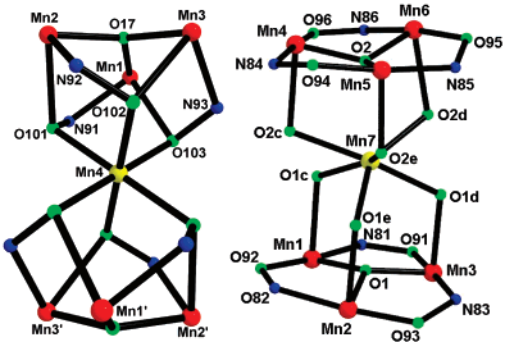

Figure 2. Core of complexes **3** (left) and **4** (right). Color code: same as that in Figure 1.

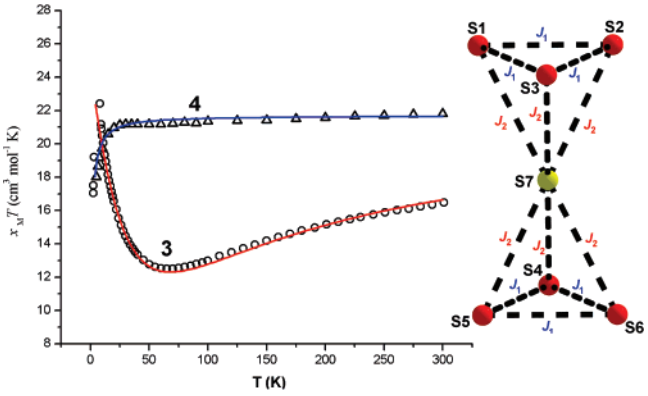

Figure 3. Left: Plot of $\chi_M T$ versus T for complexes **3** and **4**. The solid lines represent a simulation of the data in the temperature range 7−300 K. Right: Interaction scheme employed for both $[Mn_7]$ bitetrahedra (see the text for details).

Variable-temperature direct current (dc) magnetic susceptibility data were collected for both complexes in the temperature range 5.0−300 K under an applied field of 0.1 T. These are plotted as $\chi_M T$ versus T in Figure 3. For **3**, the room temperature $\chi_M T$ value of 16.47 cm^3 K mol^{-1} is lower than the expected value of 22.37 cm^3 K mol^{-1} for six Mn^{III} and one Mn^{II} noninteracting ions. Upon cooling, the value of $\chi_M T$ first decreases to 12.49 cm^3 K mol^{-1} at ∼65 K before then increasing rapidly to a maximum value of 22.42 cm^3 K mol^{-1} at 7.2 K and then decreasing to 17.11 cm^3 K mol^{-1} at 5 K. This is suggestive of the presence of competing exchange interactions, with the low-temperature maximum suggestive of an $S \approx {}^{13}/_2$ ground state. For complex **4**, the room temperature $\chi_M T$ value is 21.42 cm^3 K mol^{-1}. Upon cooling, it remains almost constant until ∼25 K, below which it decreases rapidly to a value of

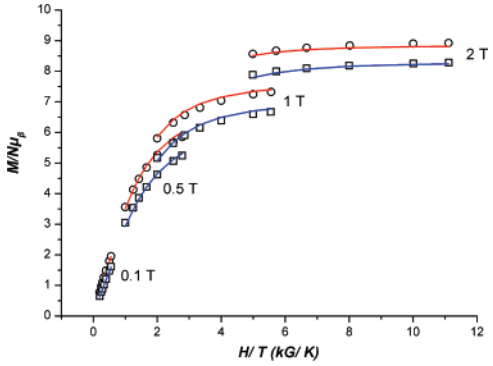

Figure 4. Plot of reduced magnetization ($M/N\mu_B$) versus H/T for **3** (circles) and **4** (squares) in the field and temperature ranges 0.1−2 T and 1.8−7 K. The solid lines correspond to the fit of the data.

18.07 cm^3 K mol^{-1} at 5 K. This value indicates an $S \approx {}^{11}/_2$ ground state. The susceptibility data for both complexes were successfully simulated using a model that employed only two J values (Figure 3): one (J_1) between the Mn^{III} ions located in the $[Mn^{III}_3O]^{7+}$ triangles (mediated by the oximate moiety of an Et-sao^{2-} ligand, the μ_3-O^{2-} ion, and the η^1:η^1:μ-acetate for **3** and the η^1:η^1:μ-ON moiety of the Et-sao^{2-} ligands, the μ_3-O^{2-} ion, and the η^1:η^1:μ-acetates for **4**) and one (J_2) between each Mn^{III} and the central Mn^{II} (mediated by a μ-oximate O atom in **3** and the η^2:η^2:μ_3-$MeCO_2^-$ in **4**). Using the program *MAGPACK*[8] and employing the Hamiltonian in eq 1

$$\hat{H} = -2J_1(\hat{S}_1\cdot\hat{S}_2 + \hat{S}_1\cdot\hat{S}_3 + \hat{S}_2\cdot\hat{S}_3 + \hat{S}_4\cdot\hat{S}_5 + \hat{S}_4\cdot\hat{S}_6 + \hat{S}_5\cdot\hat{S}_6) - 2J_2(\hat{S}_1\cdot\hat{S}_7 + \hat{S}_2\cdot\hat{S}_7 + \hat{S}_3\cdot\hat{S}_7 + \hat{S}_4\cdot\hat{S}_7 + \hat{S}_5\cdot\hat{S}_7 + \hat{S}_6\cdot\hat{S}_7) \quad (1)$$

afforded the parameters $J_1 = -2.32$ cm^{-1}, $J_2 = -4.70$ cm^{-1}, and $g = 1.95$ for **3** and $J_1 = -0.19$ cm^{-1}, $J_2 = +0.08$ cm^{-1}, and $g = 1.97$ for **4**. The ground state of **3** was found to be $S = {}^{11}/_2$ with near-degenerate $S = {}^{13}/_2$ (0.3 cm^{-1}) and ${}^{15}/_2$ (0.6 cm^{-1}) excited states, while for **4** the ground state was $S = {}^{11}/_2$ with the first and second excited states of $S = {}^{9}/_2$ and ${}^{13}/_2$ at only 0.3 and 0.4 cm^{-1} above, respectively. In theory, the model for **4** should employ three J values because the "symmetry" of the upper and lower triangles is broken via the presence of the bridging carboxylate. However, given that (a) there is some structural disorder associated with carboxylate/alcohol ligation (see the CIF files for details) and (b) employment of a three-J model did not improve the quality of the simulation or significantly change the obtained parameters, we chose not to.

In order to further verify the magnitude of the spin ground state, magnetization data were collected for both **3** and **4** in the ranges 0.1−7 T and 1.8−10 K, and these are plotted as reduced magnetization ($M/N\mu_B$) versus H/T in Figure 4. The data were fit by a matrix diagonalization method to a model that assumes that only the ground state is populated, includes axial zero-field splitting ($D\hat{S}_z^2$) and the Zeeman interaction,

(8) (a) Borrás-Almenar, J. J.; Clemente-Juan, J. M.; Coronado, E.; Tsukerblat, B. S. *Inorg. Chem.*, **1999**, *38*, 6081. (b) Borrás-Almenar, J. J.; Clemente-Juan, J. M.; Coronado, E.; Tsukerblat, B. S. *Comput. Chem*. **2001**, *22*, 985.

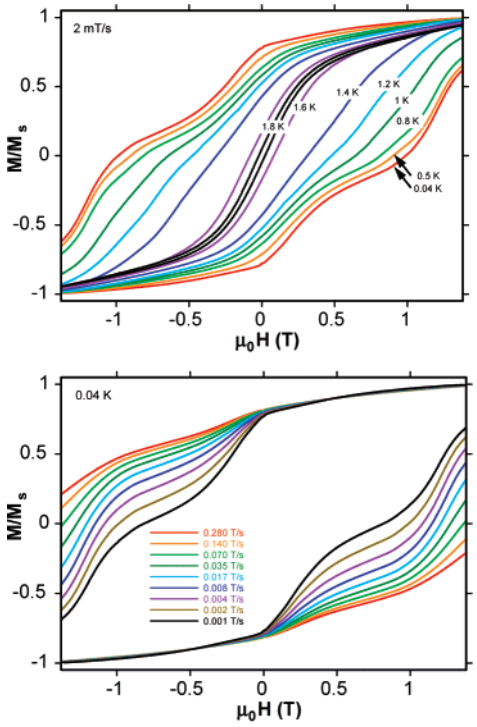

Figure 5. *M* versus *H* hysteresis loops for a single crystal of **4**. The loops are shown at different temperatures (1.8 K to 40 mK, top) and field sweep rates (0.28−0.001 T s^{-1}, bottom). *M* is normalized to its saturation value.

and carries out a full powder average. The corresponding Hamiltonian is given by eq 2, where *D* is the axial anisotropy, μ_B is the Bohr magneton, μ_0 is the vacuum permeability, $\hat{S}_z$ is the easy-axis spin operator, and **H** is the applied field.

$$\hat{H} = D\hat{S}_z^{\,2} + g\mu_B\mu_0\hat{S}\cdot H \qquad (2)$$

The best fit corresponded to the 0.1−2 T region and gave $S = {}^{13}/_2$, $g = 1.92$, and $D = -0.36$ cm^{-1} for **3** and $S = {}^{11}/_2$, $g = 1.98$, and $D = -0.39$ cm^{-1} for **4**. Using fields above 2 T, the quality of the fits become much poorer and the ground states deviate from $S = {}^{13}/_2$ (**3**) and $S = {}^{11}/_2$ (**4**) toward $S = {}^{15}/_2$ (**3**) and $S = {}^{13}/_2$ (**4**), respectively, in agreement with the susceptibility data and the presence of low-lying excited states of larger *S*. Alternating current (ac) susceptibility data were collected for both **3** and **4** in the 1.8−15 K range, under an oscillating 3.5 G field in the frequency range 50−1000 Hz. For **3**, the in-phase (χ_M') signal (Figure SI1 in the Supporting Information) increases with decreasing temperature to ∼5 K, where it then displays a frequency-dependent decrease. For **4**, the signal decreases with decreasing temperature to ∼5 K, where it then displays a frequency-dependent decrease (Figure SI2 in the Supporting Information). Extrapolation of the $\chi_M'T$ signal to 0 K from 6 K gives values of ∼23 and 18 cm^3 K mol^{-1} for **3** and **4**, respectively, indicative of $S = {}^{13}/_2$ and ${}^{11}/_2$ ground states in excellent agreement with the dc data. Out-of-phase (χ_M'') ac signals are observed for **3** (Figure SI1 in the Supporting Information) below ca. 3 K, but no peaks are observed down to 1.8 K. For **4**, the signals appear below approximately 5 K (Figure SI2 in the Supporting Information) with fully formed peaks observed for all frequencies employed; at 1000 Hz, the peak maximum occurs at ca. 3 K.

Single-crystal hysteresis loop and relaxation measurements for **3** and **4** were performed using a micro-SQUID[9] in order to conclusively prove their SMM behavior. Hysteresis loops were observed for both complexes (Figure 5 and Figure SI4 in the Supporting Information), whose coercivity was strongly temperature- and sweep-rate-dependent, increasing with decreasing temperature and increasing field sweep rate. For **3**, the tunneling at $H = 0$ is so fast it precludes the possibility of performing dc relaxation measurements, but the analogous measurements on complex **4**, combined with the above ac measurements, did allow the construction of a τ versus $1/T$ plot based on the Arrhenius relationship of eq 3, where U_{eff} is the effective relaxation barrier, τ is the relaxation time, and *k* is the Boltzmann constant (Figure SI3 in the Supporting Information). The slope of the thermally

$$\tau = \tau_0 \exp(U_{eff}/kT) \qquad (3)$$

activated region yielded an effective energy barrier for the reorientation of the magnetization of $U_{eff} \approx 32$ K and $\tau_0 = 2 \times 10^{-7}$ s. Clearly, the transverse anisotropy is much larger in the first sample, but its origin and, hence, the major difference in the observed loops, at this stage, are not easy to understand or explain.

In conclusion, the initial use of suitable countercations in the Mn/R′CO_2^-/R-saoH$_2$ reaction system has provided access to two new anionic $Mn^{III}_6Mn^{II}$ complexes that promise to be the first members of a new family of Mn SMMs. The structures of **3** and **4** are different from the general structural type reported for the $[Mn^{III}_6O_2(\text{R-sao})_6(O_2CR')_2S_x]$ family of the neutral SMMs (S = solvate molecule),[3,5] emphasizing the dependence of the product identity on small changes in the reaction conditions. The change of the coordination modes of Et-sao^{2-} and $MeCO_2^-$ from **3** to **4** demonstrates the immensely promising synthetic utility of the R′CO_2^-/R-sao^{2-} ligand combination for the generation of new Mn (and other 3d metal) clusters. Indeed, there seems to be no reason why these structures cannot be isolated with different central divalent metal ions to create a family of novel heterometallic SMMs.

Acknowledgment. This work was supported by the Leverhulme Trust and EPSRC (U.K.), the NSF (USA), and PYTHAGORAS I (Greece).

Supporting Information Available: Crystallographic details, CIF files, and magnetism data. This material is available free of charge via the Internet at http://pubs.acs.org.

IC7006638

(9) Wernsdorfer, W. *Adv. Chem. Phys.* **2001**, *118*, 99.